LAWRENCE
LIVERMORE
NATIONAL
LABORATORY

LLNL-TR-608815

Relativistic Plasma Physics at the National Ignition Facility

J. P. Palastro, T. M. Antonsen Jr.

December 19, 2012

Disclaimer

This work performed under the auspices of the U.S. Department of Energy by Lawrence Livermore National Laboratory under Contract DE-AC52-07NA27344.

Concept Development: Final Report

Relativistic Plasma Physics at the National Ignition Facility

J. P. Palastro and T.M. Antonsen Jr.

Institute for Research in Electronics and Applied Physics, University of Maryland
College Park, Maryland 20742

Introduction:

Current LPI modeling efforts are based on successful predictions of experiments at the Omega Laser Facility [1] and rely strictly on classical models for the plasma physics. The laser energy of NIF, however, is close to fifty times greater in the blue, and even higher in green. This enormous jump in laser energy catapults laser-plasma physics into uncharted territory where extrapolation from smaller facilities fails to be adequate. As an example, simulations demonstrate that the maximum electron temperature achieved in Omega hohlraums is close to 12 *keV* [2]. These hohlraums were designed especially for a high radiation temperature, resulting in the high electron temperature. Early experiments on NIF, using far less than the full laser energy, have already achieved these temperatures without having explored the temperature limits of the design space [3]. NIF is already pushing the limits of energy-density with minimal laser performance.

To this end, we have undergone a theoretical investigation of the relevant relativistic effects occurring in plasmas at energy-densities available only on NIF. In particular, we have developed a generalized, fully relativistic dispersion relation for laser plasma instabilities. The dispersion relation can provide the relativistic growth rate for any manner of parametric instability and can be considered a generalization of the well known Drake dispersion relation [4]. In addition to the inclusion of special relativity, our dispersion relation differs from the Drake dispersion relation in two key facets: we have made no assumption about the relative time scales by performing a ponderomotive average, and we have included electrostatic parametric instabilities.

Scientific Description:

The shortcoming of classical modeling in the NIF parameter regime is threefold: one, certain electromagnetic decay processes in a plasma should never be considered classical, two, as the temperature increases, the number of electrons with relativistic behavior grows exponentially, and, three, at high densities the phase velocity of a plasma wave can become relativistic. With

fully relativistic models, which can be refined and validated with optical Thomson scattering, these shortcomings can be overcome and provide more accurate analysis of the experimental data, including reflectivity measurements with FABS and NBI.

From an ignition standpoint, the hohlraum laser entrance hole (LEH) is of great interest due to symmetry tuning using cross beam energy transfer and the possibility of backward Raman amplification [5]. The LEH is also the highest temperature region of the hohlraum. Proper LPI modeling of this region, which includes the effects of relativity, is critical for backscatter mitigation, which can lead to improved design margins. Furthermore, NIF can provide more than twice the laser energy when operated with green light, making it an attractive alternative to blue, and likely the next generation option of ignition designs. With the increased energy in green light, ignition targets designs will achieve higher electron temperatures in the LEH and throughout the hohlraum. Operating with increased energy in the green also results in a higher value of $I\lambda^2$, increasing the danger of LPI, and necessitating accurate and precise models.

While relativity is a mature concept, the study of relativistic effects in hot dense-plasmas is still developing. Several fundamental relativistic concepts manifest at the energy-densities achievable on NIF: relativistic mass corrections to the electron, effective rotation of the incident electric field in the electron frame, modifications to electromagnetic force due to the relative motion of the electron and light, and collective wave effects at relativistic phase velocities. These effects alter the coupling of the laser pulse to the plasma and result in modified LPI gains. With an understanding of these effects, traditional LPI assessment tools such as PF3D and SLIP can be upgraded, and made more true-to-life.

The relativistic alterations to the classical electron motion can be observed from the force equation ($a = F/m$) for an electron in a plane electromagnetic wave

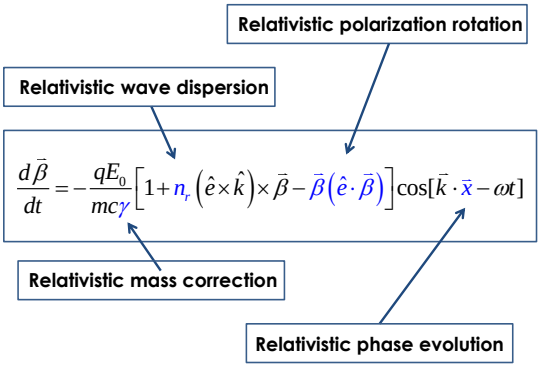

where $\vec{\beta} = \vec{v}/c$ is the normalized electron velocity, E_0 is the electric field amplitude, γ is the relativistic factor, n_r is the index of refraction of the medium, $\hat{e}$ is unit vector in the polarization direction, and $\hat{k}$ is the unit vector in the propagation direction. The occurrence of γ and $\vec{\beta}(\hat{e}\cdot\vec{\beta})$ in the force equation are clear deviations from the non-relativistic force equation. The relativistic phase evolution results from the relativistic aberrations to the

electron's trajectory, while the relativistic wave dispersion accounts for electromagnetic wave propagation in a relativistic plasma.

Neglecting relativistic modifications to the electron trajectory can result in LPI estimates with up to 100% error. In the figure below, the single particle trajectory error (the magnitude of, $[x_r(t) - x_{nr}(t)]/x_r(t)$ where the subscripts *r* and *nr* indicate relativistic and non-relativistic respectively) for an electron moving in an electromagnetic field with NIF-like laser intensities ($1\text{x}10^{15}$ W/cm^2) is plotted as a function of initial electron velocity.

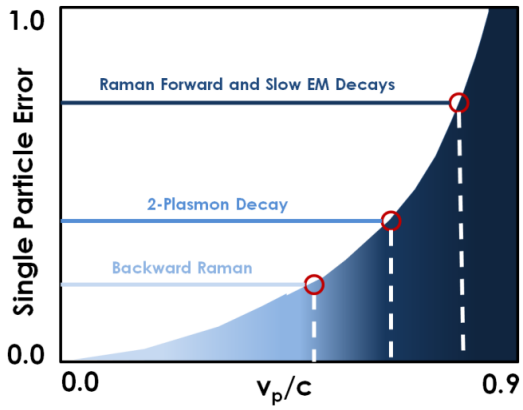

Caption, Single Particle Error: Error in using a classical equations of motion compared to relativistic for a single electron trajectory in an electromagnetic wave at different values of initial velocity, v_p. The associated velocities of the collective wave processes are demarcated. As the phase velocity increases, the error increases non-linearly.

Because the strongest interaction between the electrons and decay wave occurs when the electron velocity is matched to the phase velocity, v_p, the figure above can be considered an estimate of the error in collective wave effects. The dashed lines are typical phase velocity values for NIF parameters, demonstrating the importance of collective relativistic effects.

Results: Relativistic Dispersion Relation

We start by writing the Vlasov-Maxwell system of equations

$$\nabla\times\nabla\times\vec{E}+\frac{1}{c^2}\frac{\partial^2}{\partial t^2}\vec{E}=-\frac{4\pi}{c^2}\frac{\partial\vec{J}_p}{\partial t} \quad (1a)$$

$$\nabla\times\nabla\times\vec{B}+\frac{1}{c^2}\frac{\partial^2}{\partial t^2}\vec{B}=\frac{4\pi}{c}\nabla\times\vec{J}_p, \quad (1b)$$

$$\left[\frac{\partial}{\partial t}+c\vec{\beta}\cdot\nabla+q_s\left(\vec{E}+\vec{\beta}\times\vec{B}\right)\cdot\nabla_{\mathrm{p}}\right]F_s=0, \quad (1c)$$

where q_s and F_s are the charge and distribution function for specie s respectively. Transforming Eq. (1c) from the momentum to velocity coordinate we see the effective force in Eq. (2) resembles that appearing in the equation of motion on the previous page:

$$\left(\frac{\partial}{\partial t}+c\vec{\beta}\cdot\nabla\right)F_s=-\left(\frac{q_s}{\gamma m_s}\right)\left[\vec{E}+\vec{\beta}\times\vec{B}-\vec{\beta}\left(\vec{\beta}\cdot\vec{E}\right)\right]\cdot\nabla_{\mathrm{v}}F_s\,. \quad (2)$$

We continue by performing a Bloch-wave expansion of the electric field, magnetic field, and distribution functions

$$\vec{E}(\vec{x},t)=\vec{E}_i\sin(k_i z-\omega_i t)+\sum_\ell \vec{E}_\ell e^{i(\vec{k}_\ell\cdot\vec{x}-\omega_\ell t)}+c.c. \quad (3a)$$

$$\vec{B}=n_i\left(\hat{k}_i\times\vec{E}_i\right)\sin(k_i z-\omega_i t)+\sum_\ell n_{S,\pm}\left(\hat{k}_\ell\times\vec{E}_\ell\right)e^{i(\vec{k}_\ell\cdot\vec{x}-\omega_\ell t)}+c.c. \quad (3b)$$

$$F_s(\vec{x},\vec{\mathrm{p}},t)=f_s(\vec{\mathrm{p}})+\delta f_s(\vec{\mathrm{p}})\cos(k_i z-\omega_i t)+\sum_\ell f_{\ell,s}(\vec{\mathrm{p}})e^{i(\vec{k}_\ell\cdot\vec{x}-\omega_\ell t)}+c.c\,, \quad (3c)$$

where $n_a = c\,k_a/\omega_a$ is the index of refraction, $\mathbf{k}_l = lk_i z - \boldsymbol{\kappa}$, and $\omega_l = l\omega_i - \Omega$. The first term in Eq. (3c) represents the plasma conditions in the absence of the pump wave, which we take to be charge neutral, uniform, isotropic, and with zero flow.

The first terms in Eq. (3a) and (3b) represent the pump wave which can be electrostatic or electromagnetic. The second term In Eq. (3c) represents the standard linear change in the distribution function due to the pump wave. To lowest order we simply have the relativistic generalization of the plasma response to the pump wave. The associated dispersion relation for the pump wave is then $\varepsilon_i=0$, where

$$\varepsilon_i=1-\frac{c^2\vec{k}_i\cdot\vec{k}_i}{\omega_i^2}+\frac{c^2(\vec{k}_i\cdot\hat{e})^2}{\omega_i^2}+\frac{c}{\omega_i}\sum_s\frac{\omega_{p,s}^2}{\rho_s}\int\gamma^{-1}\beta_e D_i\vec{N}_i\cdot\nabla_{\mathrm{v}}f_s\,d\vec{\mathrm{v}}\ , \quad (4)$$

where ρ_s is the equilibrium number density of specie s, f_s is understood to now represent the velocity space distribution,

$$\vec{N}_i=(\hat{e}-\vec{\beta}\beta_e)-n_i(\hat{e}\beta_i-\hat{k}_i\beta_e)\,, \quad (5)$$

$D_a = (\omega_a - \mathbf{k}_a\cdot\mathbf{v})^{-1}$ and "^" above a variable denotes a unit vector.

Finally the summation terms in Eqs. (3a) – (3c) represent the scattered waves and nonlinear plasma response to the pump wave with for each wave. In the Bloch wave expansion each wave in the summation is a harmonic of the pump wave shifted in wavenumber and frequency. This shift in frequency, Ω, and wavenumber, $\boldsymbol{\kappa}$, is associated with the wave excited by the pump. In

particular, the l=0 term in the summation is the excited wave, while the l=+/- 1 terms represent the scattered components (stokes and anti-stokes) of the pump wave. We continue by consider these three waves. After some algebra one can find the nonlinear dispersion relation for the lowest order stokes and anti-stokes sidebands to be

$$\varepsilon_0 = \frac{\left(2\pi c E_i\right)^2}{\omega_0}\sum_{\pm}\left(\frac{1}{\omega_{\pm}}\right)\sum_n\sum_s\left(\frac{q_s^3}{m_s^2}\right)\left(\frac{q_n^3}{m_n^2}\right)\frac{\left[J^n_{0,\pm,i} \mp J^n_{0,i,\pm}\right]\left[J^s_{\pm,0,i} \pm J^s_{\pm,i,0}\right]}{\varepsilon_{\pm}} \quad (6a)$$

where ε_l is the linear dispersion relation for each wave

$$\varepsilon_\ell = 1 - \frac{c^2\vec{k}_\ell\cdot\vec{k}_\ell}{\omega_\ell^2} + \frac{c^2(\vec{k}_\ell\cdot\hat{e}_\ell)^2}{\omega_\ell^2} + \frac{c}{\omega_\ell}\sum_s\frac{\omega_{p,s}^2}{\rho_s}\int\left(\vec{e}_\ell\cdot\vec{\beta}\right)\gamma^{-1}D_\ell\vec{N}_\ell\cdot\nabla_{\mathrm{v}}f_s d\vec{\mathrm{v}} \quad (6b)$$

with the associated projection vector

$$\vec{N}_\ell = [\hat{e}_\ell - (\hat{e}_\ell\cdot\vec{\beta})\vec{\beta}] - n_\ell[\hat{e}_\ell(\hat{k}_\ell\cdot\vec{\beta}) - \hat{k}_\ell(\hat{e}_\ell\cdot\vec{\beta})] \quad (6c)$$

and resonant denominator $D_l = (\omega_l - \mathbf{k}_l\cdot\mathbf{v})^{-1}$. Finally the J functions represent kinetic coupling functions between the waves

$$J^s_{a,b,c} = \int\gamma^{-1}\left(\vec{e}_a\cdot\vec{\beta}\right)D_a\vec{N}_b\cdot\nabla_{\mathrm{v}}\gamma^{-1}D_c\vec{N}_c\cdot\nabla_{\mathrm{v}}f_s d\vec{\mathrm{v}} \quad . (6d)$$

While these expressions appear complicated, simplification results from specifying the relevant species, geometry, and phase matching conditions for the process of interest.

Results: Stimulated Raman Backward Scattering (SRS)

Of most critical importance for ignition designs is backward Raman scattering. Near the quarter critical surface of the plasma, the phase velocity of the resulting plasma wave can reach half the speed of light, requiring a relativistic treatment for accurate modeling. In this process the pump wave is electromagnetic, the scattered wave electromagnetic, and the excited wave an electron plasma wave. For simplicity we consider one dimension for which the phase matching condition can be expressed as

$$\omega_i = \omega_s + \Omega \quad (7a)$$

$$k_i(\omega_i) = k_s(\omega_s) + \kappa(\Omega) \quad (7b)$$

where s refers to the scattered wave and Ω and κ and the frequency and wavenumber of the electron plasma wave. If we consider only the resonant side band, Eq. (6a) simplifies to

$$\varepsilon_+\varepsilon_0 = \frac{\left(2\pi c E_i\right)^2}{\omega_0\omega_+}\left(\frac{q_e^6}{m_e^4}\right)\left[J^e_{0,+,i} - J^e_{0,i,+}\right]\left[J^e_{+,0,i} + J^e_{+,i,0}\right], \quad (8a)$$

where

$$\varepsilon_0 = 1 - \frac{1}{\omega_0^2}\frac{\omega_{p,e}^2}{\rho_e}\int[\alpha - 5\gamma^{-1}]\frac{\beta_i^2}{1-n_0\beta_i}\, f_e d\vec{v} \quad (8b)$$

$$\varepsilon_+ = 1 - n_+^2 - \frac{1}{\omega_+^2}\frac{\omega_{p,e}^2}{\rho_e}\int[\alpha - 5\gamma^{-1}]\frac{\beta_e^2}{1-n_+\beta_i}\, f_e d\vec{v} \quad (8c)$$

$$\vec{N}_i = (\hat{e} - \beta_e\vec{\beta}) - n_i(\hat{e}\beta_i - \hat{k}_i\beta_e) \quad (8d)$$

$$\vec{N}_0 = \hat{e}_0 - \vec{\beta}(\hat{e}_0\cdot\vec{\beta}) \quad (8e)$$

$$\vec{N}_+ = (\hat{e} - \beta_e\vec{\beta}) - n_+(\hat{e}\beta_i - \hat{k}_i\beta_e) \quad (8f)$$

and the distribution function is the Juttner [6] velocity distribution function $f_s = A\gamma^5 \exp(-\alpha\gamma)$ with $\alpha = m_e c^2/T$. While simplification has occurred the expressions for J are still quite cumbersome. We are in the process of evaluating this dispersion relation numerically in order to find the gains associated SRS and the relativistic modifications thereof.

Results: Application to Coupled Mode Equations

Finally, we have considered an extension of the relativistic dispersion relation to the coupled mode equations. Here we will consider the case of SRS. The coupled equations for the electric field amplitudes for the stokes sideband and driven wave can be expressed in the spectral domain as follows:

$$\varepsilon_+ E_+ = -\frac{2\pi c}{\omega_+}\frac{q_e^3}{m_e^2}\left[J^e_{+,0,i} + J^e_{+,i,0}\right]E_i E_0 \quad (9a)$$

$$\varepsilon_0 E_0 = -\frac{2\pi c}{\omega_0}\frac{q_e^3}{m_e^2}\left[J^e_{0,+,i} - J^e_{0,i,+}\right]E_i E_+ . \quad (9b)$$

We follow the standard technique of performing a Taylor expansion about the frequencies and wavenumbers satisfying the linear dispersion relations:

$$\varepsilon_a(\omega_a + \delta\omega_a, k_a + \delta k_a) \simeq \delta\omega_a \left.\frac{\partial\varepsilon_a}{\partial\omega_a}\right|_{\omega_a,k_a} + \delta k_a \left.\frac{\partial\varepsilon_a}{\partial k_a}\right|_{\omega_a,k_a} + \ldots \quad , (10)$$

where we have used $\varepsilon_a(\omega_a , k_a)=0$. Here $\delta\omega_a$ and δk_a represent nonlinear shifts to the frequency and wavenumber. To ensure phase matching we have $\delta\omega_0 = -\delta\omega_+$ and $\delta k_0 = -\delta k_+$. The electric field amplitudes are assumed to depend only on the non-linear frequency shifts. Upon Fourier transforming with respect to these shifts we find:

$$\left(\frac{\partial}{\partial t}-\mathrm{v}_{g,+}\frac{\partial}{\partial z}\right)E_{+}=\frac{2\pi ic}{\omega_{+}}\left[\frac{\partial\varepsilon_{+}}{\partial\omega_{+}}\right]^{-1}\frac{q_e^3}{m_e^2}\left[J^{e}_{+,0,i}+J^{e}_{+,i,0}\right]E_i E_0^{*} \quad \text{(11a)}$$

$$\left(\frac{\partial}{\partial t}-\mathrm{v}_{g,0}\frac{\partial}{\partial z}\right)E_{0}=-\frac{2\pi ic}{\omega_{0}}\left[\frac{\partial\varepsilon_{0}}{\partial\omega_{0}}\right]^{-1}\frac{q_e^3}{m_e^2}\left[J^{e}_{0,+,i}-J^{e}_{0,i,+}\right]E_i E_+^{*} \ . \quad \text{(11b)}$$

We see that the coupling coefficients for the coupled mode equations depend on the kinetic coupling functions J. Thus our relativistic dispersion relation, Eq. (6a), can provide the relativistic generalizations to the standard coupling coefficients used in programs such as pf3D or SLIP [7,8].

Conclusions:

We have derived a fully relativistic dispersion relation for nonlinear parametric processes in laser driven plasmas. The dispersion relation, while complicated, can be simplified based on the problem of interest. An example of Raman back scattering was presented. In addition we have considered the application of the dispersion relation to a set of spatio-temporal coupled mode equations. The results can be used to improve current LPI models and gain predictions for high temperature experiments on the NIF at LLNL.

Scientific Collaboration:

During this project we have collaborated with David Strozzi and Siegfried Glenzer staff scientists at LLNL in the WCI and NIF directorates respectively.

References:

[1] "Experimental basis for laser-plasma interaction predictions on the National Ignition Facility ignition designs," D.H. Froula et al., *Bulletin of the 51st annual meeting of the APS Division of Plasma Physics* Atlanta, Georgia (2009).

[2] "Plasma filling in reduced-scale hohlraums irradiated with multiple beam cones," M.B Schneider et al., *Phys. Plasmas* **13**, 112701 (2006).

[3] "Modeling laser-plasma interactions in NIF vacuum hohlraums," E.A. Williams et al., *Bulletin of the 51st annual meeting of the APS Division of Plasma Physics* Atlanta, Georgia (2009).

[4] "Parametric instabilities of electromagnetic-waves in plasmas," J. F. Drake, et al., *Phys. Fluids* **17**, 778 (1974).

[5] "Assessing the 2wpe instability and other preheat considerations in ignition-scale hohlraums," W. Kruer et al., *Bulletin of Sixth International Conference on Inertial Sciences and Applications* San Francisco, California (2009).

[6] "Relativistic Landau damping of electron plasma waves in stimulated Raman scattering," A. Bers et al., *Phys. Plasmas* **16**, 022104 (2009).

[7] "On the dominant and subdominant behavior of stimulated Raman and Brillouin scattering driven by nonuniform laser beams," R. L. Berger et al., *Phys. Plasmas* **5**, 4337 (1998).

[8] "Symmetry tuning via controlled crossed-beam energy transfer on the National Ignition Facility," P. Michel et al., *Phys. Plasmas* **17**, 056305 (2010).